Hindawi
Advances in Meteorology
Volume 2019, Article ID 3572431, 13 pages
https://doi.org/10.1155/2019/3572431

Research Article

Combination of Radar and Rain Gauge Information to Map the Snowy Region in Jeju Island, Korea: A Case Study

Jung Mo Ku[1] **and Chulsang Yoo**[2]

[1]*Research Assistant Professor, School of Civil, Environmental and Architectural Engineering, College of Engineering, Korea University, Seoul 136-705, Republic of Korea*
[2]*Professor, School of Civil, Environmental and Architectural Engineering, College of Engineering, Korea University, Seoul 136-705, Republic of Korea*

Correspondence should be addressed to Chulsang Yoo; envchul@korea.ac.kr

Received 1 February 2019; Revised 1 May 2019; Accepted 7 May 2019; Published 2 June 2019

Guest Editor: Dongkyun Kim

Hallasan Mountain is located at the center of Jeju Island, Korea. Even though Hallasan Mountain has a height of just 1,950 m, the temperature during the winter decreases below −20 degrees Celsius. On the contrary, the temperature on the coastal areas remains just above freezing. Therefore, large snowfalls in the mountain and rainfall in the coastal areas are very common in Jeju Island. Most of the rain gauges are available around highly populated coastal areas, and snow measurements are available at just four locations on the coastal areas. Therefore, it is practically impossible to distinguish the rainfall and snowfall in Jeju Island. Fortunately, two radars (Seongsan and Gosan radars) operate on Jeju Island, which fully covers Hallasan Mountain. This study proposes a method of using both the radar and rain gauge information to map the snowy region in Jeju Island, including Hallasan Mountain. As a first step, this study analyzed the Z-R and Z-S relationships to derive a fixed threshold of radar reflectivity to separate snowfall from rainfall, and, in the second step, this study additionally considered the observed rain rate information to implement the problem of using the fixed threshold. This proposed method was applied to radar reflectivity data collected during November 1, 2014, to April 30, 2015, and the results indicate that the method considering both the radar and rain gauge information was satisfactory. This method also showed good performance, especially when the rain rate was very low.

1. Introduction

Mapping the snowy region is very important in our daily lives. In some places it rains, but in other places, maybe in high-elevation areas, it can snow. If it snows, it may be necessary to limit vehicle traffic, remove snow from the road and roadsides, and sometimes warn climbers against trespassing. Accurately predicting the snowline is thus important, especially where the rainfall and snowfall simultaneously occur.

Jeju Island, which is located in the southernmost part of the Korean Peninsula, is likely the only place where both rainfalls in the plain coastal area and the snowfall in mountainous areas can be observed at the same time. This is mainly because Hallasan Mountain is located at the center of Jeju Island. With a height of 1,950 m, Hallasan Mountain is known to have a strong orographic precipitation. During winter, from December to February, the mean temperature in the coastal area is around 6.5~7.3°C, but that in the mountain area decreases to around −2.3~1.0°C. At the mountain top, the temperature easily drops below −10°C [1].

There are two main roads in Jeju Island: one is the beltway along the sea shore and the other an expressway that connects two big cities, Jeju City and Seogwipo City, in Jeju Island. In particular, the expressway passes the side of Hallasan Mountain at an elevation of 700 m. Unfortunately, this expressway is frequently closed due to heavy snowfall during the winter. Four access roads to Hallasan Mountain run up to an elevation of 1,000 m.

However, in Jeju Island, it is practically impossible to divide areas of the rainfall and snowfall. The Jeju Regional Meteorological Administration (JRMA) operates a total of 24 rain gauges, but 13 rain gauges are located near the sea

shore (elevation 0 to 250 m from the sea level) where the population is high. Rain gauges in the high-elevation mountain area are very limited. Snowfall observations are carried out at four locations over Jeju Island (Jeju, Seogwipo, Seongsan, and Gosan), but these are all in the coastal areas where snowfall is very rare. Rain gauges in the mountainous area can measure snowfall according to water depth, but it is not easy to distinguish snowfall from rainfall.

Radar data may be used as an alternative to divide areas between the rainfall and snowfall. Basically, radar reflectivity on rain drops is different from that on snow flakes. For example, the Z-R relationships between the radar reflectivity (Z) and rain rate (R, mm/hr) are $Z = 200R^{1.6}$ [2], $Z = 31R^{1.71}$ [3], $Z = 486R^{1.37}$ [4], etc. On the contrary, the Z-S relationships between radar reflectivity (Z) and snow rate (unit of mm/hr, the same as R) are $Z = 2{,}000S^{2.0}$ [5], $Z = 2{,}100S^{2.0}$ [6], $Z = 427S^{1.09}$ [7], etc. The two relationships are markedly different in their proportional constants, i.e., the proportional constant of the Z-S relationship is generally much larger than that of the Z-R relationship.

However, the problem is that, for a given radar reflectivity, it is impossible to distinguish the snowfall and rainfall. This is the main issue in this study. Currently, classification of rainfall and snowfall fully relies on the information of air temperature. It is generally assumed that snow cannot exist if the temperature is higher than 5°C [8]. Also, the guideline from the Korean Meteorological Administration (KMA) shows that the precipitation is assumed to be snowfall if the temperature is lower than 1.2°C [9]. So the problem is that the range between the obvious rainfall and obvious snowfall is too wide. This range of temperature corresponds to the elevation difference around 500 m. In case the prediction of snowline much matters such as in Jeju Island, the temperature information may not be a sufficient indicator.

The objectives of this study are as follows. First, this study will analyze the Z-R and Z-S relationships reported so far worldwide to characterize their difference. The difference between the two may give us an idea of separating the snowfall from rainfall. Second, as the known range of radar reflectivity of rainfall is much wide and includes that of the snowfall, simply a fixed radar reflectivity value may not be useful to map the snowy region [10]. In this case, additional information must be used to successfully achieve the study objective. In this study, rain gauge data will be considered as secondary information to separate snowfall from rainfall, as it is generally accepted that radar reflectivity is proportional to the rain rate.

This manuscript is composed of a total of five sections, including Introduction and Conclusions. In the second section, the Z-R and Z-S relationships are reviewed to derive their difference. In the third section, the study area and the data are explained. Finally, the fourth section explains the methodology and application examples using the data collected by both radar and rain gauges in Jeju Island, Korea.

2. Z-R and Z-S Relationships

The equation for the so-called Z-R relationship has the following form [11]:

$$Z = AR^b, \tag{1}$$

where Z is the radar reflectivity (mm^6/m^3), R is the rain gauge rain rate (mm/hr), and A and b are parameters. These two parameters are known to vary so widely regionally and depending on storm types. Table 1 introduces some Z-R relationships collected from past studies and reports worldwide.

Similar to the Z-R relationship to estimate the radar rain rate from the radar reflectivity, the so-called Z-S relationship is used to estimate the radar snow rate [15]. The basic form of the equation for the Z-S relationship is the same as that for the Z-R relationship:

$$Z = AS^b, \tag{2}$$

where the snow rate S has the same unit of mm/hr as the rain rate. Table 2 shows some Z-S relationships collected from past studies and reports. In this table, Z_e has the relation with Z such as $Z_e = 0.244 \times Z$. This relation was proposed in [22] for melted snowflakes.

The variability of the parameters for the Z-R and Z-S relationships is quite different from each other. Figure 1 compares the box plots of parameters A and b of the two relationships collected in this study. As can be seen in this figure, the range of parameter A of the Z-R relationship is 16.6~730 and that for parameter b is 1.0~2.87. On the contrary, the range of parameter A of the Z-S relationship is 160~3,300 and that for the parameter b is 1.09~2.21; that is, the ranges of parameter A are very different, but those of parameter b are similar to each other.

Simply plotting the Z-R relationships and Z-S relationships collected in this study produces Figure 2. The log-log scale was used in this figure, so all relationships are shown linearly over the Z-R and Z-S planes. Comparing these two panels, one can easily find that the slopes of the lines are similar to each other. In fact, this is a natural result because parameter b is similar in both relationships. However, the intercept, which is related to parameter A, is found to be very different from each other.

This study used the concept of a confidence interval to summarize the Z-R relationships and Z-S relationships. In general, the confidence interval is derived as a fixed one about the given mean. However, in this study, the confidence interval was derived for the entire range of the radar reflectivity as a function of R or S. The radar reflectivity Z for a given R or S was assumed to follow the Gaussian distribution. The 95% confidence intervals (i.e., 2.5~97.5% range) derived for the Z-R relationship and Z-S relationship also overlapped in Figures 2(a) and 2(b), respectively. As can be seen in a comparison of these two confidence intervals, Z for S is distinctly higher than that for R. However, it is also true that these two confidence intervals overlap a bit to make a separation of snowfall from rainfall become very complicated.

3. Study Area and Data

3.1. Study Area. Jeju Island is located in the southernmost region of the Korean Peninsula. In fact, Jeju Island is composed of the main island, eight inhabited islands, and 55

Table 1: Z-R relationships collected from past studies and reports.

Precipitation type	Z-R relationship	Reference
Stratiform	$Z = 200R^{1.60}$	[2]
Convective	$Z = 16R^{1.55}$	[3]
All storms	$Z = 372R^{1.47}$	[4]
Thundershowers	$Z = 435R^{1.48}$	
Rainshowers	$Z = 370R^{1.31}$	
Continuous	$Z = 311R^{1.43}$	
Cold front	$Z = 208R^{1.39}$	[12]
Continuous	$Z = 322R^{1.33}$	[13]
Warm air advection	$Z = 207R^{1.50}$	[14]
Cold air advection	$Z = 205R^{1.50}$	
Weak gradient type	$Z = 201R^{1.50}$	
Thunderstorms	$Z = 291R^{1.50}$	
Warm air advection	$Z = 183R^{1.50}$	
Cold air advection	$Z = 200R^{1.50}$	
Weak gradient type	$Z = 191R^{1.50}$	
Thunderstorms	$Z = 254R^{1.50}$	
Warm air advection	$Z = 200R^{1.50}$	
Cold air advection	$Z = 255R^{1.50}$	
Weak gradient type	$Z = 206R^{1.50}$	
Thunderstorms	$Z = 318R^{1.50}$	

Table 2: Z-S relationships collected from past studies and reports.

Precipitation type	Z-S relationship	Z_e-S relationship	Reference
Snowflakes	$Z = 500S^{1.60}$	$Z_e = 112S^{1.60}$	[16]
	$Z = 1{,}800S^{1.60}$	$Z_e = 403S^{1.60}$	
	$Z = 1{,}200S^{1.60}$	$Z_e = 269S^{1.60}$	
Snowflakes	$Z = 2{,}000S^{2.0}$	$Z_e = 448S^{2.0}$	[5]
Snowflakes			[6]
Dry ($\overline{T} < 0^\circ$)	$Z = 540S^{2.0}$	$Z_e = 120S^{2.0}$	
Wet ($\overline{T} > 0^\circ$)	$Z = 2{,}100S^{2.0}$	$Z_e = 470S^{2.0}$	
Snowflakes	$Z = 1{,}780S^{2.21}$	$Z_e = 399S^{2.21}$	[17]
Snowflakes consisting of the following crystal types:			
Plates and columns	$Z = 400S^{1.60}$	$Z_e = 60S^{1.60}$	[18]
Needle crystals	$Z = 930S^{1.90}$	$Z_e = 208S^{1.90}$	
Stellar crystals	$Z = 1{,}800S^{1.50}$	$Z_e = 403S^{1.50}$	
Spatial dendrites	$Z = 3{,}300S^{1.70}$	$Z_e = 739S^{1.70}$	
Single crystals	$Z = 160S^{2.0}$	$Z_e = 36S^{2.0}$	[19]
Snowflakes			[20]
Dry ($\overline{T} < 0^\circ$)	$Z = 1{,}050S^{2.0}$	$Z_e = 235S^{1.60}$	
Wet ($\overline{T} > 0^\circ$)	$Z = 1{,}600S^{2.0}$	$Z_e = 358S^{1.60}$	
Snowfall (1 g = 0.03 mm/h)	$Z = 427S^{1.09}$	$Z_e = 96S^{1.09}$	[7]
Hail	$Z = 320S^{1.60}$	$Z_e = 72S^{1.60}$	[21]
Graupel	$Z = 900S^{1.60}$	$Z_e = 202S^{1.60}$	

$\overline{T}$ = mean air temperature.

uninhabited islands. Figure 3 shows Jeju Island and its administrative districts.

Jeju Island is a volcanic island composed of about 360 small-scale volcanoes and volcanic cones [1]. Hallasan Mountain is located at the center of Jeju Island, and it sits at a height of 1,950 m. Hallasan Mountain has a gentle slope of about 3° along the east–west direction, but a steeper slope of about 5° along the north–south direction (Jeju Special Self-Governing Province, http://www.jeju.go.kr). The shape of the island is elliptical, with a major axis length of 73 km along the east–west direction and a minor axis length of 31 km along the north–south direction. The total area for Jeju Island is 1,848 km^2, and the coastal area whose elevation above the sea level is less than 200 m covering 55.3% of the island's total area.

3.2. Rain Gauge and Radar Data. In 1990, the Korea Meteorological Administration (KMA) started to introduce automated weather stations (AWSs) in Jeju Island [23]. Now, a total of 24 AWSs are in operation [24]. Among them, 16 rain gauges are located in the coastal area with an elevation of less than 250 m, four in between 250 and 500 m,

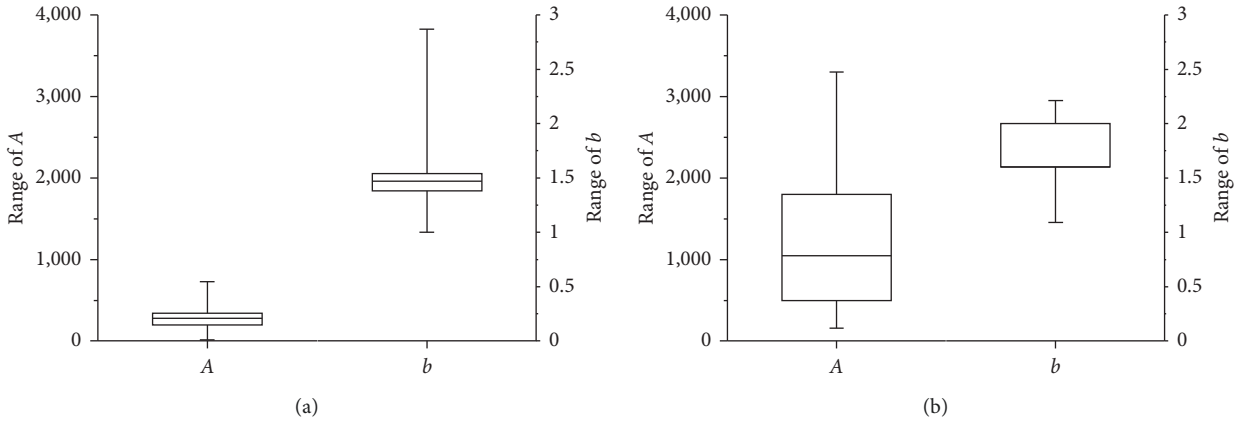

Figure 1: Comparison of the (a) *Z*-*R* and (b) *Z*-*S* relationships with their box plots of parameters *A* and *b*.

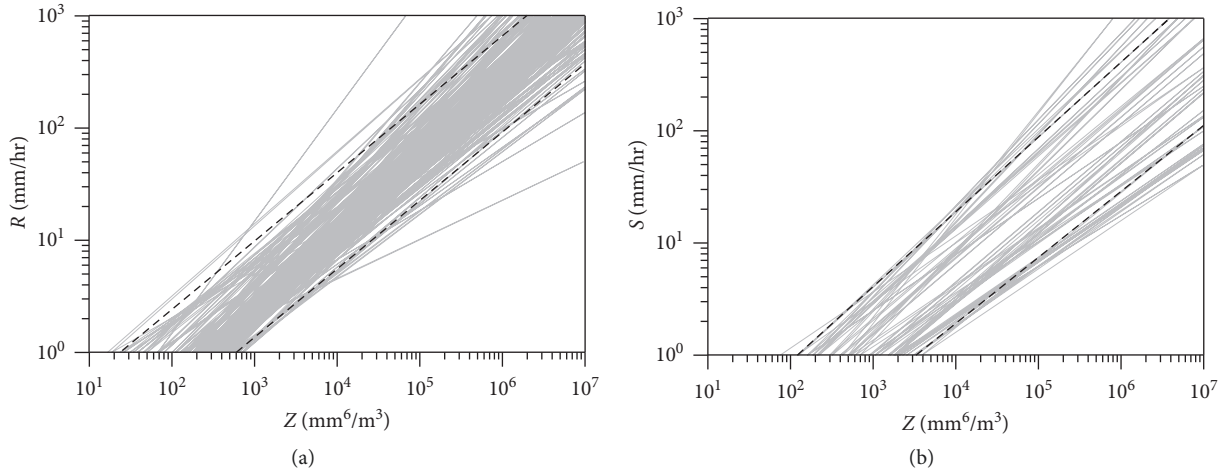

Figure 2: 95% confidence intervals derived for the (a) *Z*-*R* and (b) *Z*-*S* relationships.

two in between 750 and 1,000 m, one in between 1,250 and 1,500 m, and one at 1,500 m or higher. The locations of the rain gauges are shown in Figure 4.

KMA operates the Gosan radar and Seongsan radar in Jeju Island. The Gosan radar, which was originally a C-band radar, started tracking typhoons in 1991 but was replaced by an S-band radar in 2006. The Seongsan radar was introduced in 2006 to supplement the Gosan radar, specifically to remove the blind spot caused by Hallasan Mountain. Seongsan radar is also an S-band radar, and both radars possess an observation radius of 240 × 240 km and a resolution of 1 × 1 km. The major specifications of the Gosan and Seongsan radars are summarized in Table 3.

From both the Gosan and Seongsan radars, a total of eight radar reflectivity fields were prepared from an elevation of 250 m to 2,000 m in intervals of 250 m. That is, from each radar, 0.25 km CAPPI, 0.50 km CAPPI, 0.75 km CAPPI, 1.00 km CAPPI, 1.50 km CAPPI, 1.75 km CAPPI, and 2.00 km CAPPI data were prepared. These data were used to produce a composite field at each elevation. When data were available from both radar systems, their arithmetic mean was calculated to make the representative reflectivity. The radar reflectivity data that were used were captured from November to April from 2007 to 2016. A total of 21 AWSs data were used in Jeju Island during the same period.

4. Mapping the Snowy Region

4.1. Using Only the Radar Information. In this study, the mapping of the snowy region was first attempted based on the difference between the *Z*-*R* and *Z*-*S* relationships. The radar reflectivity data were collected for the winter period from the year 2007 to 2016. In most cases, the data collected in the coastal area are for the rainfall and those in the mountain area the snowfall. However, as the snowline varies so widely in both space and time, it is not easy to separate the snowfall from rainfall simply by analyzing the radar reflectivity value. In this study, among the data collected, those within the 95% significance range of *Z*-*R* relationship were selected, as shown in Figure 5(a), for the elevation zone of 250–500 m, as an example. Those within the 95% significance range of the *Z*-*S* relationship were also selected, as shown in Figure 5(b). Even though it was impossible to check if these two datasets were really rainfall or snowfall,

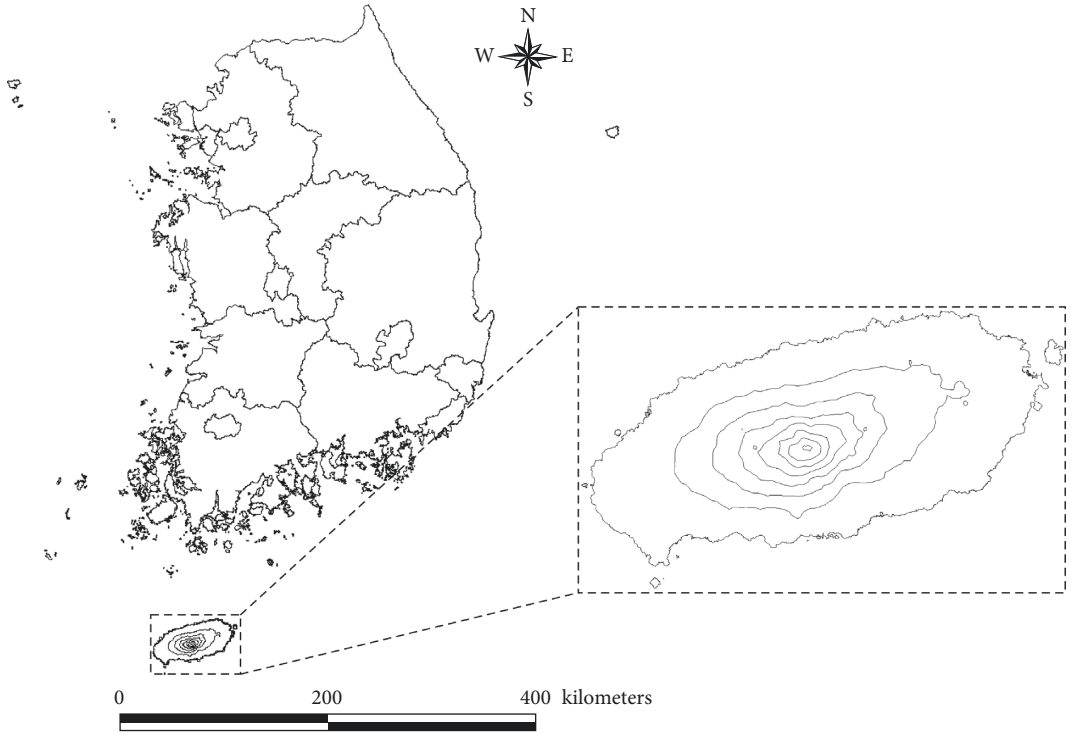

Figure 3: Location of Jeju Island, Korea (the contour lines over Jeju Island represent the 250 m altitude interval).

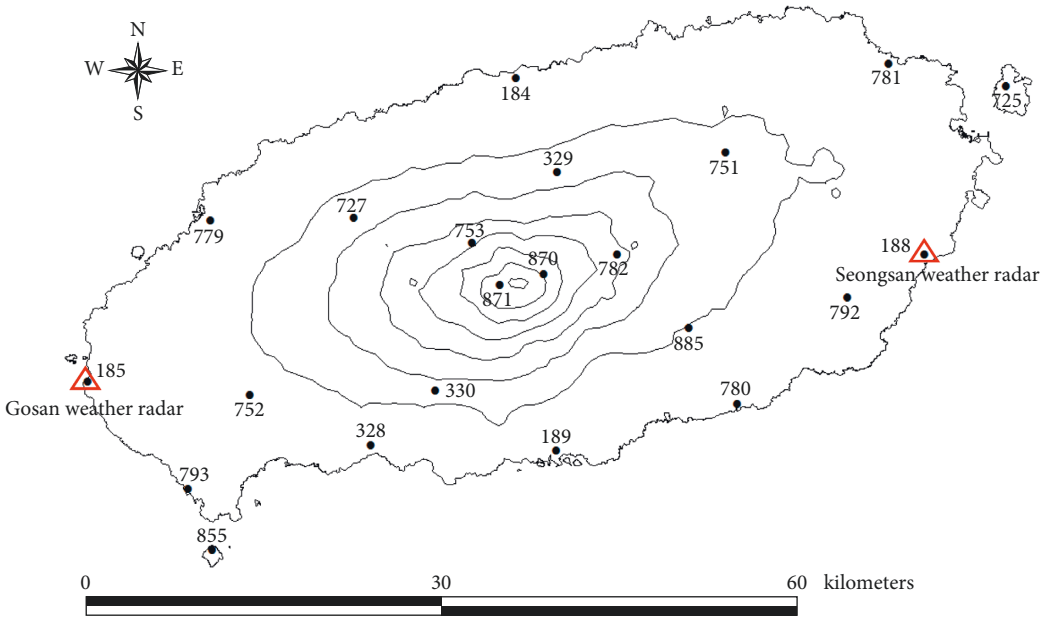

Figure 4: Locations of rain gauges over Jeju Island and two radars located at Gosan and Seongsan, Jeju Island.

they were assumed so at this point. These two datasets were then quantified by probability density functions (Figure 6). Here the Gaussian distribution was assumed since the dBZ unit was used for the radar reflectivity [25–27]. For the rainfall case, radar reflectivity data were distributed over a range of 20 to 50 dBZ but for the snowfall over the range of 30 to 55 dBZ. They obviously overlapped, indicating the possibility of uncertainty in the separation of snowfall from rainfall.

As can be seen in Figure 6, the mean of the radar reflectivity for the rainfall was 26.1 dBZ and that, for the snowfall case, was 41.8 dBZ. Their standard deviations were similar at 5.6 dBZ and 6.6 dBZ, respectively. The range of overlapping radar reflectivity for both the rainfall and snowfall was found to be between 24 and 42 dBZ. Theoretically, both the rainfall and snowfall can happen if the radar reflectivity is within this range. However, its possibility

Table 3: Major specification of the Gosan and Seongsan radars.

	Radar type		Gosan radar S band	Seongsan radar S band
Transmitter	Transmitting tube		Klystron	Klystron
Receiver	Frequency		2,825 MHz	2,755 MHz
	Peak power		750 kW	750 kW
	Pulse width	Short	1.0 μs	1.0 μs
		Long	4.5 μs	4.5 μs
	PRF	Short pulse	250~1,200 Hz	250~1,200 Hz
		Long pulse	250~350 Hz	250~350 Hz
	Occupied bandwidth		8 MHz	8 MHz
Antenna	Dynamic range		95 dB	95 dB
	Intermediate frequency		10 MHz	10 MHz
	Antenna diameter		8.5 m	8.5 m
	Beam width		1.0°	1.0°
	Antenna gain		45 dB	45 dB

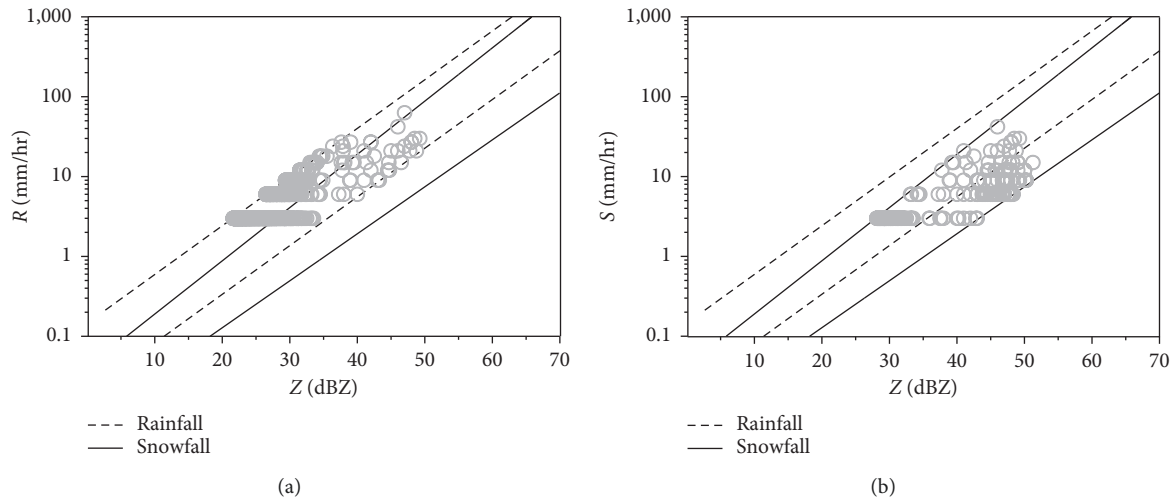

Figure 5: Comparison of observed (a) rainfall and (b) snowfall data along with their radar reflectivity collected over the elevation zone of 250~500 m (data collected during winter from 2007 to 2016).

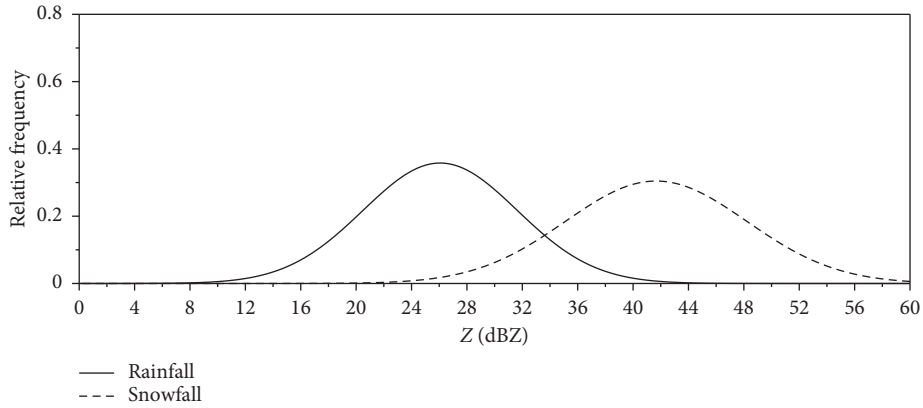

Figure 6: Comparison of probability density functions for rainfall and snowfall data over the elevation zone of 250~500 m.

(or the probability) is totally different. Near the low bound of this range, it is more like the rainfall, and near the upper bound of this range, it is more like the snowfall. In this study, the concept of a contingency table was used to determine the threshold value of the radar reflectivity to separate the rainfall and snowfall conditions. A contingency table is composed of four different probabilities indicating the true and false probabilities under the assumption of rainfall or snowfall.

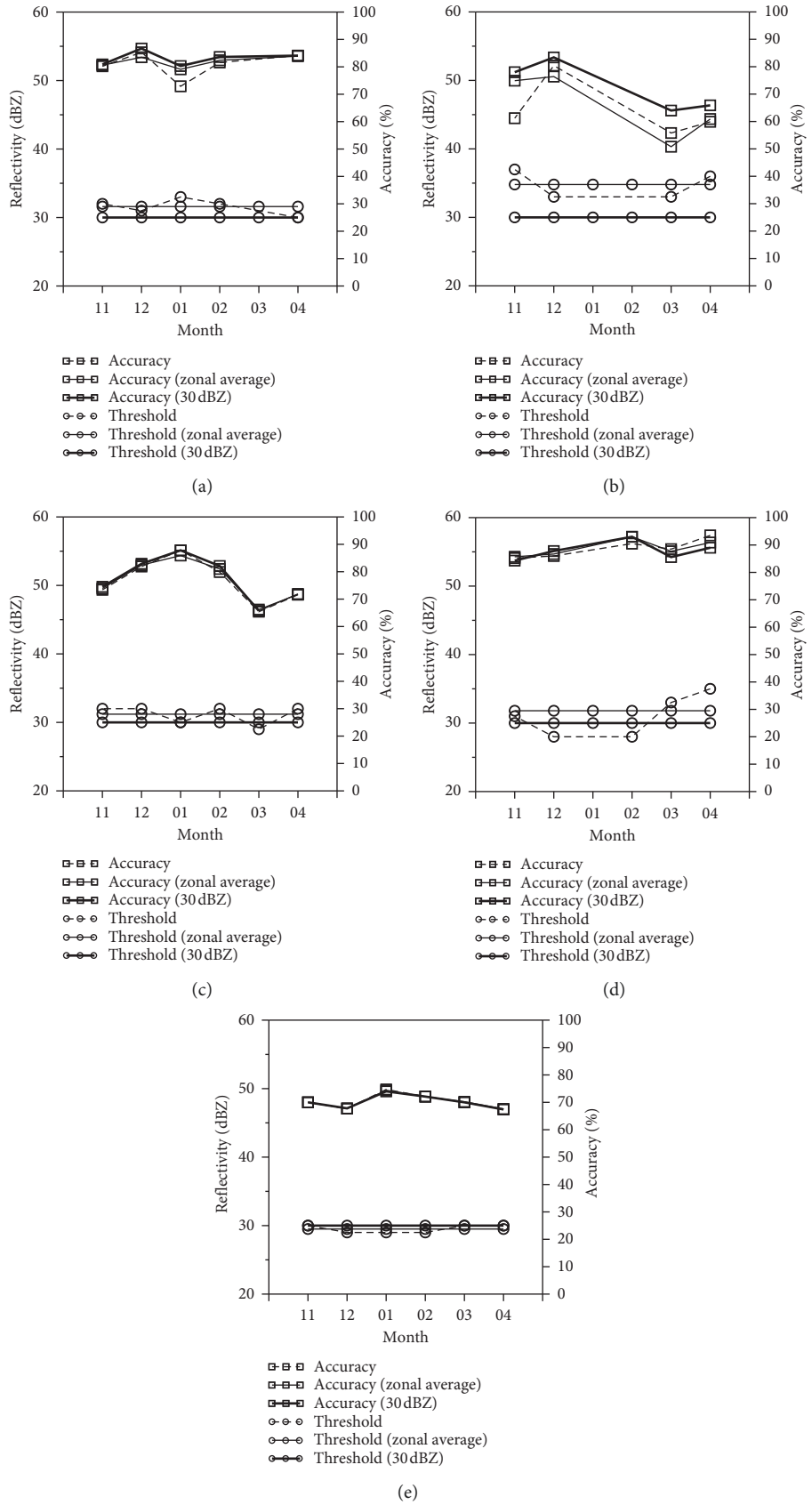

Figure 7: Monthly variation of the threshold radar reflectivity value (○) and its accuracy (□) for each elevation zone (the zonal-average threshold value and fixed threshold value (30 dBZ) are also given for the comparison): (a) 1,750 m; (b) 1,500 m; (c) 1,000 m; (d) 500 m; (e) 250 m.

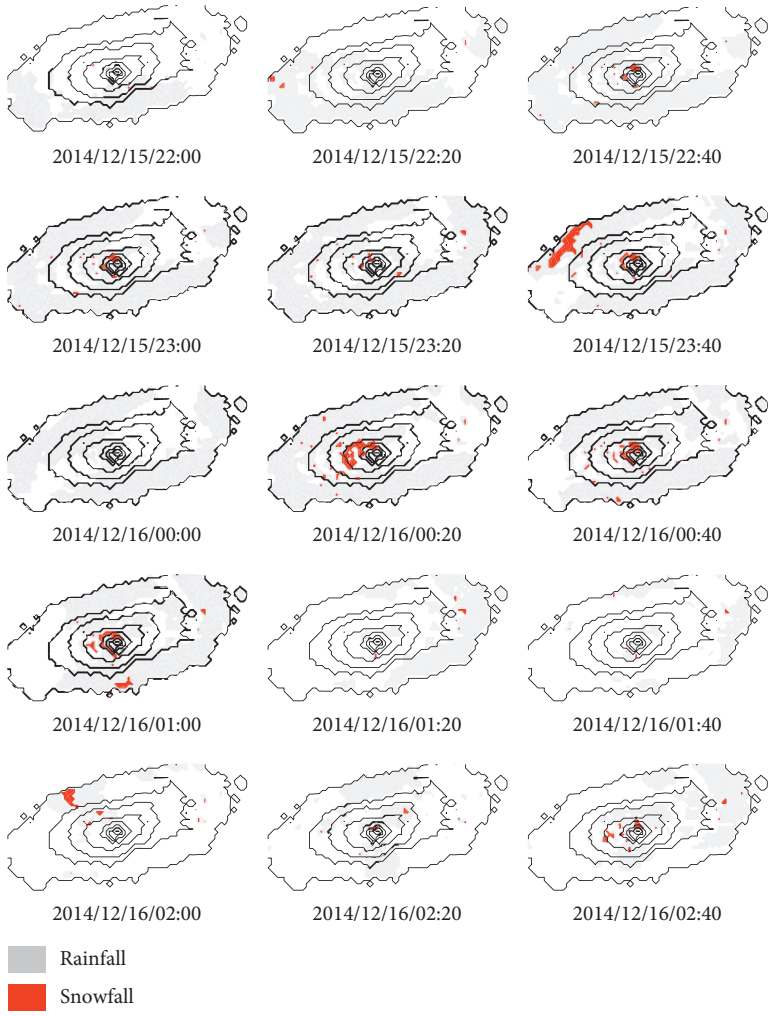

Figure 8: Mapping result of the snowy region by applying the fixed threshold method (from 22:00 December 15 to 02:40 December 16, 2015).

By changing the threshold value of the radar reflectivity, the average accuracy of rainfall and snowfall predictions as well as their difference was calculated. It is obvious that the accuracy of the rainfall prediction increases as the threshold value decreases. On the contrary, the accuracy of the snowfall prediction increases as the threshold value increases. Thus, the average accuracy should be determined somewhere in between the low and high threshold values, which was around 33~35 dBZ in this case. However, the difference in the accuracy between the rainfall and snowfall prediction was the smallest at a threshold value of 33 dBZ, which increased rather highly as the threshold value increased. Since both the average accuracy and the difference in the accuracy between the rainfall and snowfall prediction were important, this study determined the threshold value to be 33 dBZ.

Following the same procedure, this study determined the threshold value for each elevation zone from November to April, when the snowfall is observed in the mountain area of Jeju Island. The results are summarized in Figure 7. In this figure, the symbol "○" represents the threshold values, and the symbol "□" represents the average accuracy. This figure shows that the threshold values that were determined monthly were more or less the same at most elevation zones except for the elevation zone of 250~500 m. Even in the elevation zone of 250~500 m, the threshold value remained similarly from November to February, but it increased a bit from March. In the case of applying a fixed threshold value for each elevation zone, the average accuracy was found not to change significantly from that estimated by applying the value determined monthly (Figure 7). It is also noticeable that the threshold values were all determined at around 30 dBZ regardless of the elevation. Thus, this study decided to use the fixed threshold value of 30 dBZ to map the snowy region for every month and the elevation zones considered in this study. By applying this fixed threshold value, the accuracy deteriorates slightly, as shown in Figure 7.

Next, this study attempted to map the snowy region with a fixed threshold of the radar reflectivity value of 30 dBZ to the radar reflectivity data measured over Jeju Island from November 1, 2014, to April 30, 2015. As an example, Figure 8 shows the mapping results from 22:00 December 15 to 02:40 December 16, 2015. In this figure, the red colour represents the snowy region and the grey colour the rainy region.

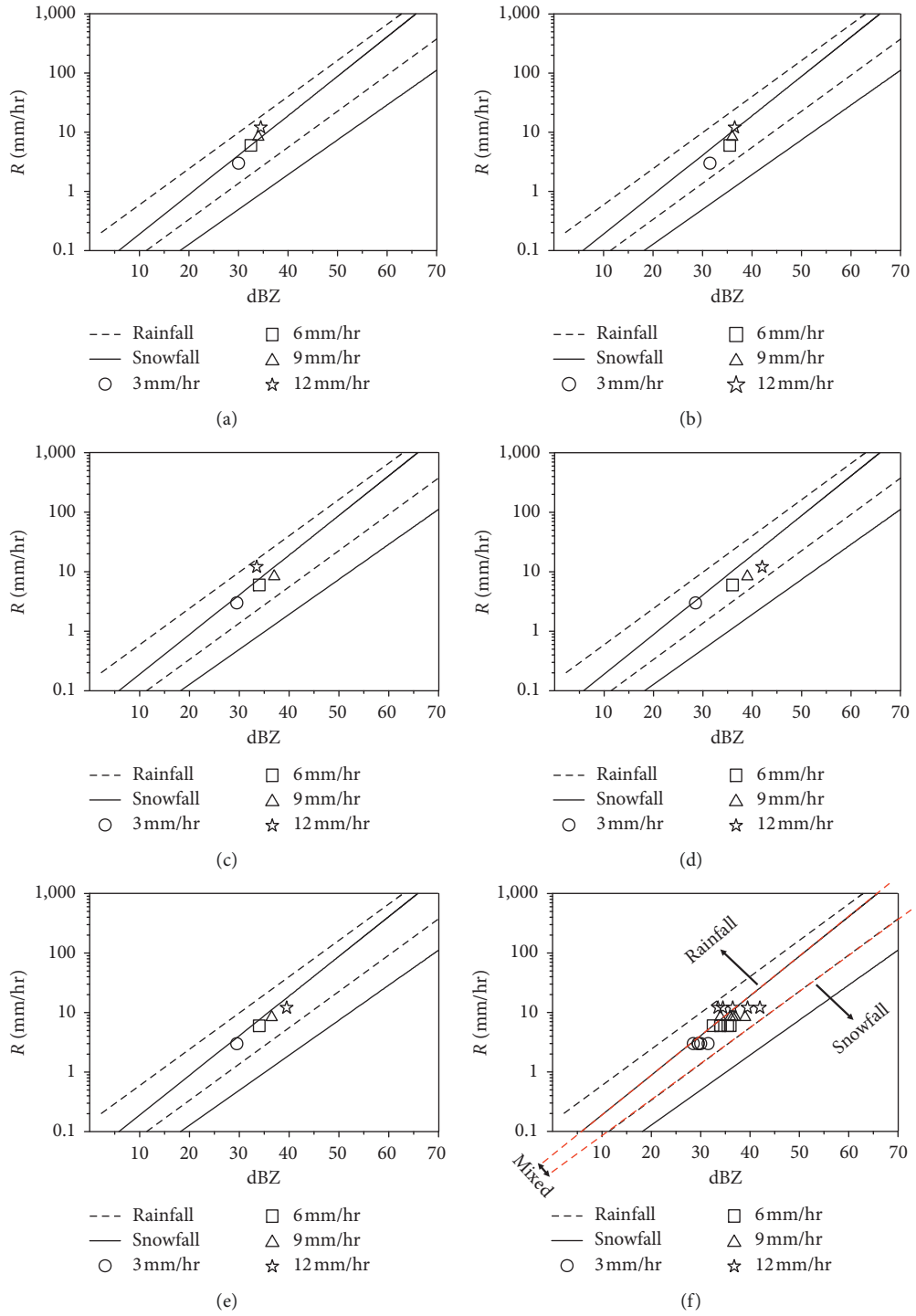

FIGURE 9: The threshold radar reflectivity values for snowfall determined by considering the rain gauge data in each elevation zone ((a)–(e)) and the overall result (f): (a) 1,750 m; (b) 1,500 m; (c) 1,000 m; (d) 500 m; (e) 250 m; (f) overall.

At this moment, it is not certain if the mapping result is correct or not. As the snowfall did not accumulate in the low elevation zone (the atmospheric temperature is generally above zero), the result could not be confirmed based on the snowfall measurements at four locations located in the low elevation zone of 0 to 250 m. However, Figure 8 shows that the snowy region occurred rather randomly over the Jeju Island, which is also inconsistent with the atmospheric temperature. Higher elevation zones were classified as the snowy zone, but some low elevation zones were also classified as the snowy zones even when the temperature was rather high. Overall, it is true that the mapping result contains lots of uncertainty. The behavior of snowfall in space is random, and also the mapping result lacks the physical consistency with the atmospheric temperature.

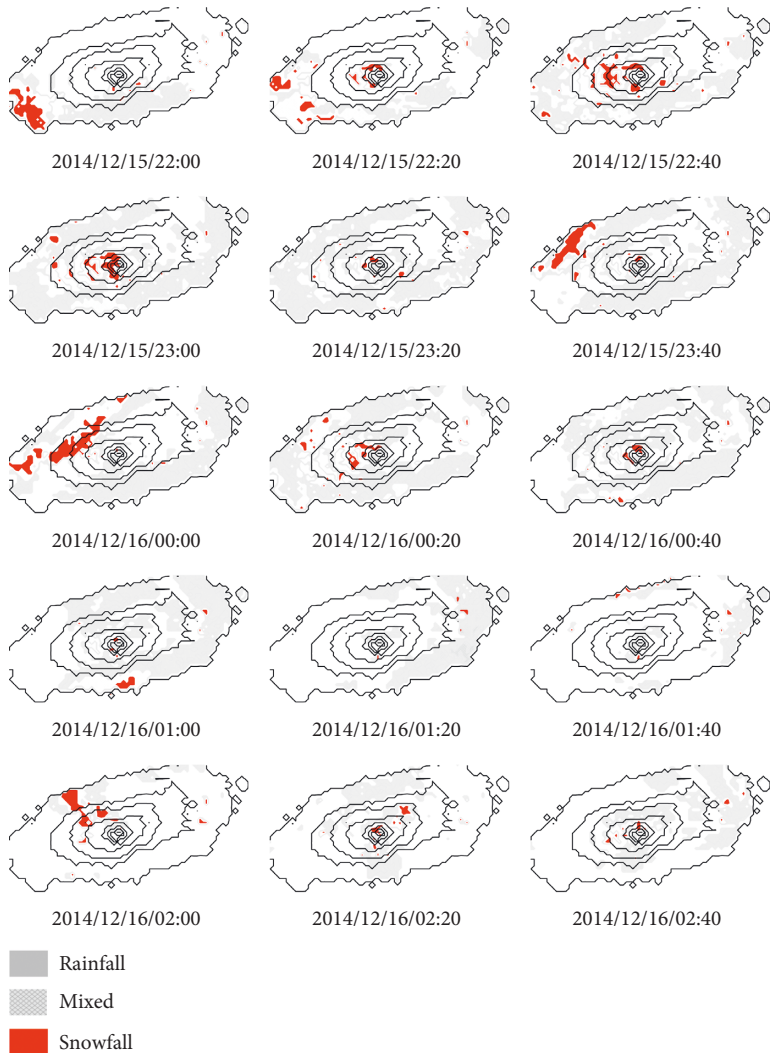

Figure 10: Mapping result of the snowy region by applying the variable threshold method (from 22:00 December 15 to 02:40 December 16, 2015).

4.2. Using Both the Radar and Rain Gauge Information. The radar reflectivity is proportional to the rain rate (=rainfall depth/duration) or snow rate (=snowfall depth/duration). Thus, in this study, to consider this behavior of the radar reflectivity, another method was proposed to additionally consider the rain rate data measured at each ground rain gauge station. All the rain gauges in Jeju Island are equipped with a melting device for snow and thus can measure the snowfall by units of rain rate. The monthly variation of the threshold value was not considered in this study, as it was found to be very small in the analysis in the previous section.

First, in this study, the threshold values were estimated again using the observed radar and rain gauge data by additionally considering the rain rate (or the snow rate). Since the rain rate during the winter was so low, only four ranges of the rain rate could be considered, which are 0~3.0 mm/hr, 3.0~6.0 mm/hr, 6.0~9.0 mm/hr, and 9.0~12.0 mm/hr. Figure 9 shows the results for each elevation zone given over the 95% significance interval derived in the previous section. As can be seen in this figure, in all elevation zones, the threshold radar reflectivity was determined to be proportional to the rain rate. The threshold values were also found to be all within the overlapping zone of confidence intervals of Z-R and Z-S relationships. In particular, the threshold values were found to be located nearer to the upper bound of the 95% confidence interval of the Z-S relationship.

Based on above result, the study decided to use the upper bound of the 95% confidence interval of the Z-S relationship as the threshold for snowfall. Similarly, as the threshold for rainfall, the lower bound of the 95% confidence interval of the Z-R relationship was used. In between the two thresholds, a zone of the mixed rainfall and snowfall was assumed.

Next, this proposed method with a variable threshold was applied with the same data considered in the previous section. As was explained earlier, the variable threshold of the radar reflectivity was derived by considering the rain rate. Both thresholds for the rainfall and snowfall were defined, and additionally, the zone for the mixed rainfall and

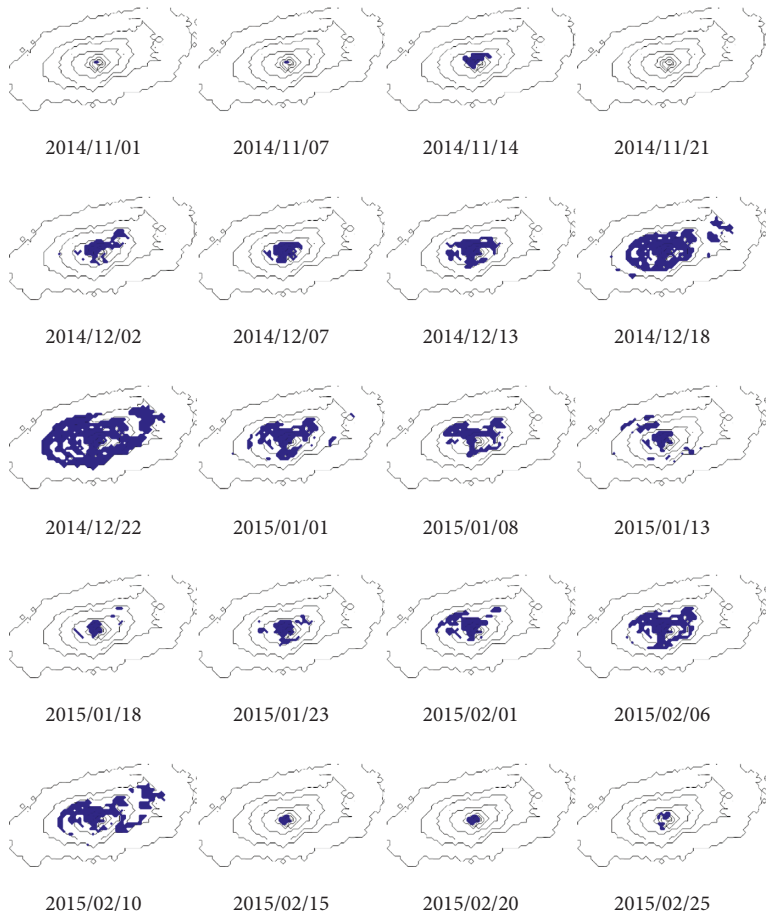

Figure 11: Change of the snow coverage over Jeju Island from November 1, 2014, to February 25, 2015, determined by applying the variable threshold method.

snowfall was also introduced to consider the uncertainty of classifying the rainfall and snowfall. An example applying the variable threshold method to the event observed on 22:00 December 15 to 02:40 December 16, 2015, is given in Figure 10. In this figure, the red colour indicates the snowfall and grey colour indicates rainfall. Additionally, the cross stripes represent the mixed rainfall and snowfall.

Different from previous results in Figure 8, Figure 10 shows somewhat distinct features. First, the snowy region in this case was larger than that in the previous case. If adding the area for the mixed rainfall and snowfall, the snowy region becomes much larger than that in the previous case. Second, especially on the top of Hallasan Mountain at subzero temperatures, radar reflectivity data were also classified into either snowfall or mixed. In the previous case, most of the radar reflectivity data in the high-elevation zone was classified into rainfall. Third, the behavior of a snow storm, i.e., directional property of the snowfall movement, could be clearly identified. In this example, the snowfall approached from the west or northwest to Jeju Island, which also scattered snowfall mostly on the rising limb of Hallasan Mountain. This behavior of the snowfall could not be detected when applying the fixed threshold method. Obviously, the variable threshold method showed a superior performance to classify the rainfall and snowfall. In addition, applying the variable threshold method was also found to be advantageous, especially when the rain rate was very low.

4.3. Determination of the Snowline at Hallasan Mountain, Jeju Island. Finally, in this study, the snowline of Hallasan Mountain was determined by applying the variable threshold method. The snowline in this case indicates the lowest elevation where snow is observed. In this study, snow was assumed to melt away if the temperature was higher than 5°Celsius [8], and that snow would disappear regardless of the snow depth. As an example, Figure 11 shows the change in the snow coverage over Jeju Island from 250 m to 2,000 m. At the early stages of winter, snow was detected around the top of Hallasan Mountain, but the snow-covered area increased significantly during winter and then decreased again at the end of the winter.

To determine the snowline, snowfall ratios of 10% and 90% were considered in this study (Figure 12). The snowfall ratio was calculated by dividing the number of snowy cells by the total number of cells at each elevation zone. In fact, the criterion 10% was a very weak one but was considered to show the snow-detectable elevation and its change during the winter. The second case was added to estimate the number of days when the snow-covered Hallasan Mountain

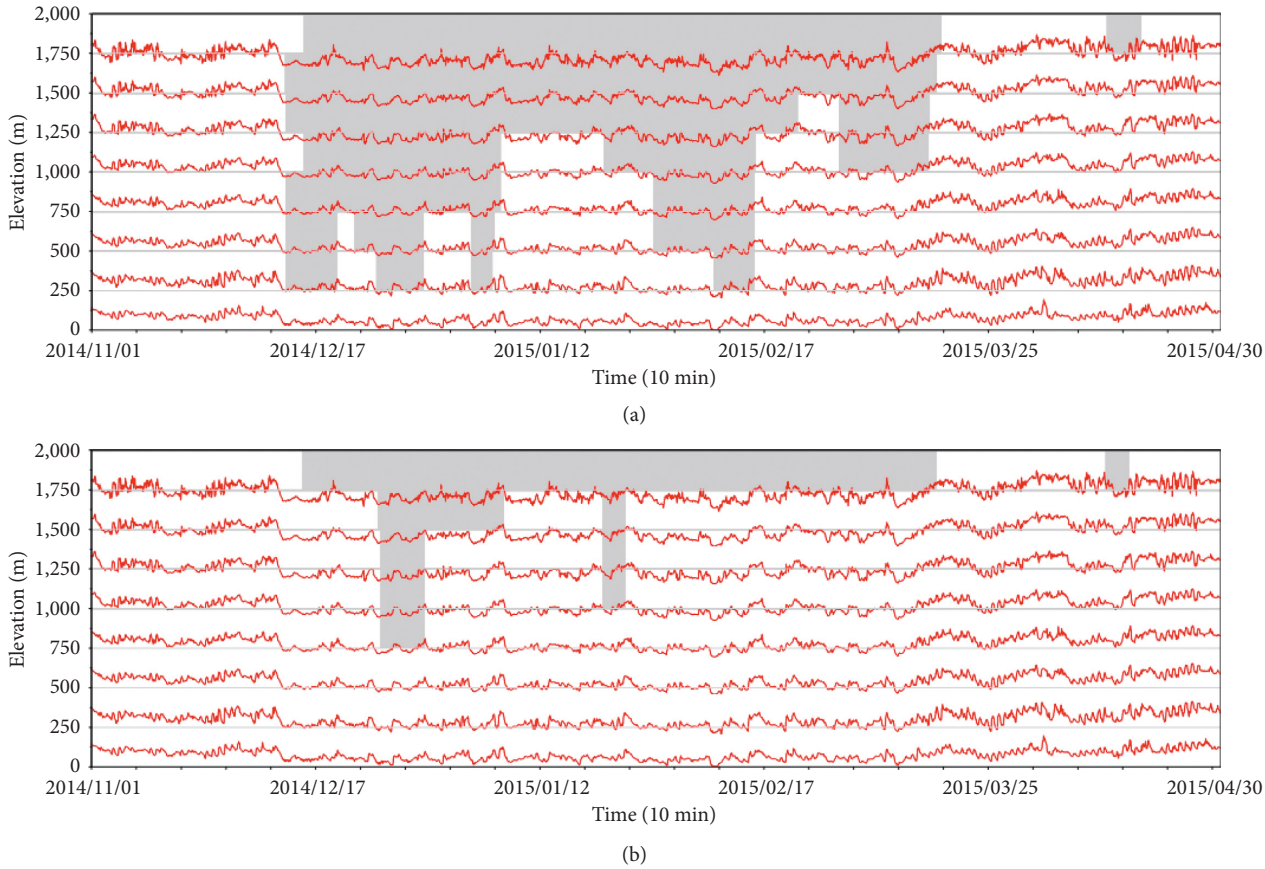

Figure 12: Change of the snowline (shaded area) over Jeju Island from November 1, 2014, to April 30, 2015, determined by applying the variable threshold method ((a) snow coverage 10% or higher; (b) snow coverage 90% or higher). Also, the thin wiggly line represents the air temperature measured at each elevation, which is moving around the reference temperature 0°C (i.e., the horizontal line at each elevation).

could be seen. The result shows that the snowy mountain top can be seen from December to the beginning of March in Jeju Island.

5. Summary and Conclusions

In this study, a method was proposed to map the snowy region using both the radar and rain gauge information. As a first step, this study analyzed the *Z*-*R* and *Z*-*S* relationships to derive a fixed threshold of radar reflectivity to separate snowfall from rainfall, and in the second step, this study additionally considered the observed rain rate information to address the problem of using the fixed threshold. This proposed method was applied to radar reflectivity data collected during November 1, 2014, to April 30, 2015, in Jeju Island, Korea. The results are summarized as follows.

For the case of using only the radar information, the threshold value of the radar reflectivity was determined to be 33 dBZ. However, the application of this threshold value did not show any satisfactory results. The results showed that the snowy region occurred rather randomly, which was also inconsistent with the atmospheric temperature.

For the case of using both the radar and rain gauge information, the threshold radar reflectivity was determined to be proportional to the rain rate. The threshold values were especially found nearer to the upper bound of the 95% confidence interval of the *Z*-*S* relationship. Similarly, as the threshold for the rainfall, the lower bound of the 95% confidence interval of the *Z*-*R* relationship was determined for use. Between the two thresholds was assumed to be the zone of the mixed rainfall and snowfall. Application of this proposed method resulted in somewhat distinct features like (1) obvious snowfall on the top of Hallasan Mountain in subzero temperature and (2) directional property of the snowfall movement. This method based on the variable threshold depending on the rain rate showed a superior performance in classifying the rainfall and snowfall, including a good performance particularly when the rain rate was very low.

Based on above results, the proposed method in this study based on the variable threshold value of radar reflectivity considering the observed rain rate could be confirmed to be effective when applied to map the snowy region. Especially, the AWS, which can measure the snowfall by the unit of water depth, was found to be beneficial to improve the quality of snowfall prediction. Even though this is a case study over Jeju Island, Korea, the same methodology may be applied anywhere with a similar environment. Especially, this methodology can be advantageous in the mountainous areas where snow measurements are not systematically taken.

Data Availability

The radar data and ground data used in this study were collected from the Korean Meteorological Administration (https://data.kma.go.kr).

Conflicts of Interest

The authors declare that they have no conflicts of interest regarding the publication of this paper.

Acknowledgments

This work was supported by the "Basic Science Research Program," through the National Research Foundation of Korea, funded by the Ministry of Education (NRF-2016R1D1A1A09918155), and the Korea Environment Industry & Technology Institute (KEITI) of the Korea Ministry of Environment (MOE) through "Advanced Water Management Research Program" (79615).

References

[1] Jeju Regional Meteorological Administration, *Detailed Climate Characteristics of Jeju Island*, Jeju Regional Meteorological Administration, Jeju, South Korea, 2010.

[2] J. S. Marshall and W. M. K. Palmer, "The distribution of raindrops with size," *Journal of Meteorology*, vol. 5, no. 4, pp. 165-166, 1948.

[3] D. C. Blanchard, "Raindrop size-distribution in Hawaiian rains," *Journal of Meteorology*, vol. 10, no. 6, pp. 457–473, 1953.

[4] D. M. A. Jones, *Research Report: Rainfall Drop-Size Distribution and Radar Reflectivity*, Illinois State Water Survey Meteorology Laboratory, Champaign, IL, USA, 1956.

[5] K. L. S. Gunn and J. S. Marshall, "The distribution with size of aggregate snowflakes," *Journal of Meteorology*, vol. 15, no. 5, pp. 452–461, 1958.

[6] I. Imai, "Raindrop size distributions and the *Z-R* relationship," in *Proceedings of the 8th Weather Radar Conference*, pp. 321–326, American Meteorological Society, Boston, MA, USA, 1960.

[7] Y. Fujiyoshi, T. Endoh, T. Yamada, K. Tsuboki, Y. Tachibana, and G. Wakahama, "Determination of a *Z-R* relationship for snowfall using a radar and high sensitivity snow gauges," *Journal of Applied Meteorology*, vol. 29, no. 2, pp. 147–152, 1990.

[8] The Korean Earth Science Society, *Concepts in Earth Science*, The Korean Earth Science Society, Seoul, South Korea, 2005.

[9] National Institute of Meteorological Research, *Development of Advanced Atmospheric Technology (III)*, National Institute of Meteorological Research, Seoul, South Korea, 2011.

[10] J. H. Lee and C. S. Ryu, *Radar Meteorology*, Sigma Press, Seoul, South Korea, 2009.

[11] J. O. Laws and D. A. Parsons, "The relation of raindrop-size to intensity," *Transactions, American Geophysical Union*, vol. 24, no. 2, pp. 452–460, 1943.

[12] R. Cataneo and G. E. Stout, "Raindrop-size distributions in humid continental climates, and associated rainfall rate-radar reflectivity relationships," *Journal of Applied Meteorology*, vol. 7, no. 5, pp. 901–907, 1968.

[13] G. E. Stout and E. A. Mueller, "Survey of relationships between rainfall rate and radar reflectivity in the measurement of precipitation," *Journal of Applied Meteorology*, vol. 7, no. 3, pp. 465–474, 1968.

[14] I. G. Doelling, J. Joss, and J. Riedl, "Systematic variations of *Z-R*-relationships from drop size distributions measured in northern Germany during seven years," *Atmospheric Research*, vol. 47-48, pp. 635–649, 1998.

[15] J. S. Marshall and K. L. S. Gunn, "Measurement of snow parameters by radar," *Journal of Meteorology*, vol. 9, no. 5, pp. 322–327, 1952.

[16] I. Imai, M. Fujiwara, I. Ichimura, and Y. Toyama, "Radar reflectivity of falling snow," *Papers in Meteorology and Geophysics*, vol. 6, no. 2, pp. 130–139, 1955.

[17] R. S. Sekon and R. C. Srivastava, "Snow size spectra and radar reflectivity," *Journal of the Atmospheric Sciences*, vol. 27, no. 2, pp. 299–307, 1970.

[18] T. Ohtake and T. Henmi, "Radar reflectivity of aggregated snowflakes," in *Proceedings of the 14th Conference on Radar Meteorology*, pp. 209-210, American Meteorological Society, Tucson, AZ, USA, 1970.

[19] P. E. Carlson and J. S. Marshall, "Measurement of snowfall by radar," *Journal of Applied Meteorology*, vol. 11, no. 3, pp. 494–500, 1972.

[20] T. Puhakka, "On the dependence of the *Z-R* relation on the temperature in snowfall," in *Proceedings of the 16th Conference on Radar Meteorology*, pp. 504–507, American Meteorological Society, Houston, TX, USA, 1975.

[21] R. Rasmussen, M. Dixon, S. Vasiloff et al., "Snow nowcasting using a real-time correlation of radar reflectivity with snow gauge accumulation," *Journal of Applied Meteorology*, vol. 42, no. 1, pp. 20–36, 2003.

[22] P. L. Smith, "Equivalent radar reflectivity factors for snow and ice particles," *Journal of Climate and Applied Meteorology*, vol. 23, no. 8, pp. 1258–1260, 1984.

[23] G. Choi, "Spatial patterns of seasonal extreme precipitation events in Mt. Halla," *Journal of Climate Research*, vol. 8, no. 4, pp. 267–280, 2013.

[24] National Geographic Information Institute, *The Geography of Korea—Jeju Special Self-Governing Province*, National Geographic Information Institute, Suwon, South Korea, 2013.

[25] J. A. Smith and W. F. Krajewski, "Estimation of the mean field bias of radar rainfall estimates," *Journal of Applied Meteorology*, vol. 30, no. 4, pp. 397–412, 1991.

[26] D.-J. Seo, J. P. Breidenbach, and E. R. Johnson, "Real-time estimation of mean field bias in radar rainfall data," *Journal of Hydrology*, vol. 223, no. 3-4, pp. 131–147, 1999.

[27] S. Chumchean, A. Seed, and A. Sharma, "Correcting of real-time radar rainfall bias using a Kalman filtering approach," *Journal of Hydrology*, vol. 317, no. 1-2, pp. 123–137, 2006.